Beyond superwetting surfaces: dual-scale hyperporous membrane with rational wettability for "non-fouling" emulsion separation via coalescence demulsification

Jianqiang Wang,[ab], Bing He,[ac] Yajie Ding,[a] Tiantian Li,[a] Weilin Zhang,[a] Yingjie Zhang,[c] Fu Liu,*[ab] and Chuyang Y. Tang[d]*

[a] Key Laboratory of Marine Materials and Related Technologies, Zhejiang Key Laboratory of Marine Materials and Protective Technologies, Ningbo Institute of Materials Technology and Engineering, Chinese Academy of Sciences, Ningbo, 315201, P. R. China
E-mail: wangjianqiang@nimte.ac.cn; fu.liu@nimte.ac.cn

[b] University of Chinese Academy of Sciences, Beijing, 100049, P. R. China

[c] School of Marine Science and Technology, Sino-Europe Membrane Technology Research Institute, Harbin Institute of Technology, Weihai, 264209, P. R. China

[d] Department of Civil Engineering, The University of Hong Kong, Hong Kong, 999077, P. R. China

ABSTRACT: Membrane fouling is the obstacle that limited the practical application of membranes for efficient oil/water separation. The main reason for membrane fouling is the deposition of dispersed phase (e.g. oil) on membrane surface based on sieving effect. The key challenge for solving fouling problem is to achieve fouling removal via rationally considering hydrodynamics and interfacial science. Herein, poly(vinylidene fluoride) (PVDF) membrane with dual-scale hyperporous structure and rational wettability is designed to achieve a continuous "non-fouling" separation for oil/water emulsions via membrane demulsification. The membrane is fabricated via dual phase separation (vapor and non-solvent) and modified by *in situ* polymerization of poly(hydroxyethyl methylacrylate) (PHEMA) (contact angle 59 ± 1°). The membrane shows stable permeability (1078±50 $Lm^{-2}h^{-1}bar^{-1}$) and high separation efficiency (>99.0%) in 2 h of continuous cross flow without physicochemical washing compared to superwetting membranes. The permeation is composed of two distinct immiscible liquid phases via coalescence demulsification. Surface shearing and pore throat collision coalescence demulsification mechanism is proposed, and rational interface wettability facilitates the foulants/membrane interaction for "non-fouling" separation. Beyond superwetting surfaces, a new strategy for achieving "non-fouling" emulsion separation by designing membranes with dual-scale hyperporous structure and rational wettability is provided.

KEYWORDS: *beyond superwetting surfaces, non-fouling emulsion separation, coalescence demulsification, PVDF membrane.*

■ INTRODUCTION

Nowadays, oily wastewaters generated from industry discharges, ocean oil spills and human's daily lives have posed serious threat to the health of human beings and ecosystem. [1-2] Many strategies have been proposed to deal with oily wastewaters. [3-6] Membrane separation technique shows its superiority over others due to its high separation efficiency, cost effectiveness and physical nature of separation. [7-8] However, the troublesome fouling issue, which reduces membrane permeability, limits its continuous and long-term separation in practical applications. [9-10] Therefore, realization of "non-fouling" oil/water emulsion separation through innovative design of membranes and separation processes is a research priority.

Different from molecular and colloidal foulant deposition during other pressure-driven membrane separation processes (e.g., reverse osmosis and nanofiltration [11]), fouling during oil/water separation was attributed to the adsorption, accumulation and adhesion of micrometer-scale dispersed phases (e.g. oil or water). [12-13] Moreover, fouling becomes dramatically severe in the presence of surfactants, [14-15] and therefore high frequency of physical and chemical cleaning is usually required, which burdens the separation process. [16-17] In order to alleviate membrane fouling, great efforts have been devoted to constructing superwetting membranes by manipulating surface energy and roughness. [18-21] Despite all these notable progresses, [22-31] membrane fouling issue cannot be solved once and for all. The retention mechanism based on sieving effect resulted in inevitable fouling intrinsically. The dispersed oil phase is rejected and concentrated on feed side while continuous phase passing through the membrane as filtrates. Despite low adhesion of superwetting surfaces, the intercepted oils tend to coalesce and adhere to the surface as oily film, which blocks the water passage and deteriorates the membrane permeability. [32-35] Therefore, superwetting membranes

are not sufficient to guarantee enduring and antifouling oil/water separation.

Some novel separation processes have emerged recently, such as Janus membrane with unidirectional property for oil/water separation. [36-38] This process allows dispersed phases to diffuse and permeate through the membrane via capillary force while continuous phases are rejected. However, permeability of dispersed phase is often limited (30~60 $Lm^{-2}h^{-1}$) because of slow diffusion process. [39-41] Except for the single phase removal strategy, actually simultaneous permeation of dispersed and continuous phases was also reported. [42-43] During this process, dispersed oil phases are intercepted and coalesces on the hydrophobic surface of membrane, and are subsequently dragged out of membrane by the continuous phase. [44] However, the highly hydrophobic membrane makes it difficult to detach the coalesced oil due to high adsorption, which aggregates the membrane fouling. In addition, hydrophobic membrane will cause high intrusion pressure and thus adversely affect the water permeability. Therefore, effective removal of dispersed phase away from membrane surface or tortuous pores is the preferential consideration for oil/water separation. Membrane demulsification gives us a promising solution to "non-fouling" and enduring oil/water separation. The micro-emulsion can go through the membrane and evolve into macroscopic coalesced phase through membrane demulsification during this process. Beyond superwetting surfaces, rational design of membrane structure and wettability is prerequisite to achieve "non-fouling" separation via membrane demulsification.

In this study, we achieved a continuous oil/water separation process with negligible fouling via membrane demulsification. We rationally fabricated hyperporous poly(vinylidene fluoride) (PVDF) membrane with dual-layer micro/nano scale pore structure and rational surface hydrophilicity (water contact angle 59±1°) via vapor/non-solvent induced phase separation and *in situ* incorporation of hydrophilic PHEMA (Figure 1). The hyperporous

structure brings about coalesced demulsification of oil/water emulsions and rational hydrophilic surface/interface and offers anti-fouling transportation of micro/macroscopic droplets through the tortuous pathways. The rationally designed PVDF membrane constantly maintains stable permeability (1078±50 $Lm^{-2}h^{-1}bar^{-1}$) with high separation efficiency (> 99%) for toluene-in-water emulsion in 2 h of continuous cross-flow filtration. The surface shearing and throat-pore squeezing coalescence mechanism was proposed to elucidate membrane demulsification. Highly hydrophilic and hydrophobic membranes were evaluated for oil/water separation as control samples to show the anti-fouling capability of rationally hydrophilic surface/interfaces. This study gives us a promising solution to "non-fouling" separation of oil/water emulsions beyond common superwetting membranes.

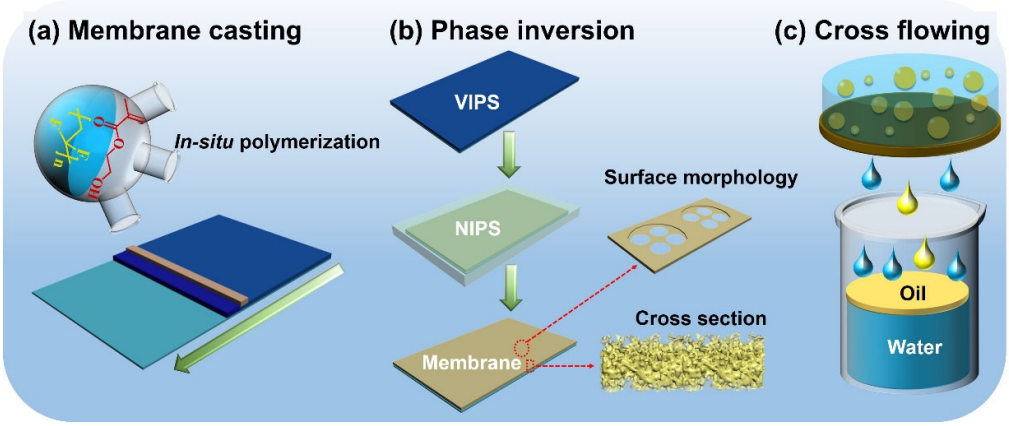

Figure 1. Schematic diagram of the membrane fabrication and membrane demulsification process: a) PVDF solution with *in situ* polymerized PHEMA was casted on non-woven fabrics, b) the nascent membrane undergoes dual phase separation (vapor and non-solvent) to acquire dual-scale hyperporous structure and controlled wettability, c) rationally designed membrane shows demulsified separation for oil/water emulsion under cross-flow filtration.

■ RESULTS AND DISCUSSION

Dual-scale hyperporous membrane. In Figure 2, surface of PVDF(H)-N_5 exhibits a dual-layer hyperporous structure that is distinctly different from those accessible with conventional

approaches. Vapor and TEP/water induced phase separation was utilized to construct the exterior primary microscale pore and interior secondary nanoscale pore structure. Interestingly, the instant residence (5 s) in TEP/water gives rise to the circular micropores (Figure 2b) on the surface compared to PVDF(H)-N_0 and PVDF(H)-N_{60} (Figure 2a, c). Below the exterior layer, the interior bulk exhibits tortuous spongy-like pores (Figure 2d, e, f, Figure S2). In Figure 2h, the dual-layer surface of PVDF(H)-N_5 displays a bimodal pore size distribution with primary pores (0.5-2.5 μm) and secondary pores (0.1-0.3 μm), in contrast to PVDF(H)-N_0 and PVDF(H)-N_{60} with unimodal pore distribution in the range of 0.1-0.3μm (Figure 2g and 2i). The patterned circular micropore structure was generated by the dual-phase separation process. Saturated vapor was cooled, absorbed and condensed on the surface of the nascent film, and then arranged in an ordered pattern due to the Marangoni effect. [45] Subsequently, the doping of TEP in water decreased the surface tension of condensed micro-droplets, delayed the phase inversion and promoted the formation of exterior porous skin layer. Eliminating TEP or extending residence duration cannot maintain the metastable state of condensed droplets and therefore common unimodal pore distribution surface was obtained. Moreover, incorporation of hydrophilic PHEMA facilitated the formation of breath figure patterns in aspect of thermodynamics and mass transfer kinetics. Hydrophilic domains could decrease vapor-liquid interface tension and promote micro-phase separation between PVDF and PHEMA due to hydrophobic/hydrophilic incompatibility. [46-47] For comparison, PVDF membranes without involving PHEMA showed irregular porous surface despite vapor exposure and varying residence time in TEP/water (Figure S3).

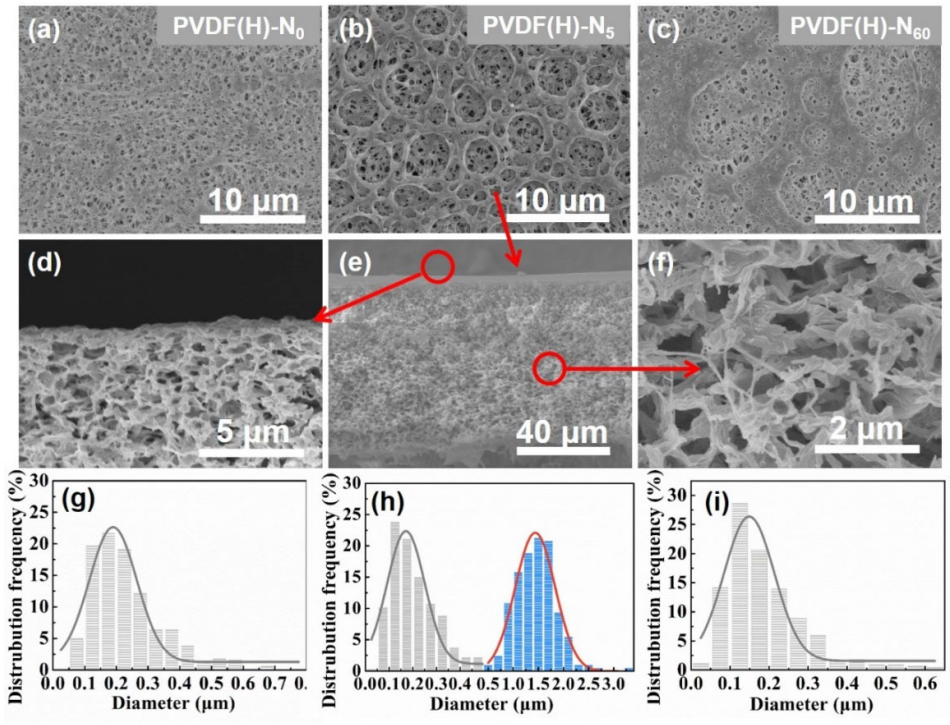

Figure 2. Surface SEM images of a) PVDF(H)-N_0, b) PVDF(H)-N_5, c) PVDF(H)-N_{60} and d-f) cross-sectional SEM images of PVDF(H)-N_5 membrane. Pore size distribution of g) PVDF(H)-N_0, h) PVDF(H)-N_5 and i) PVDF(H)-N_{60}.

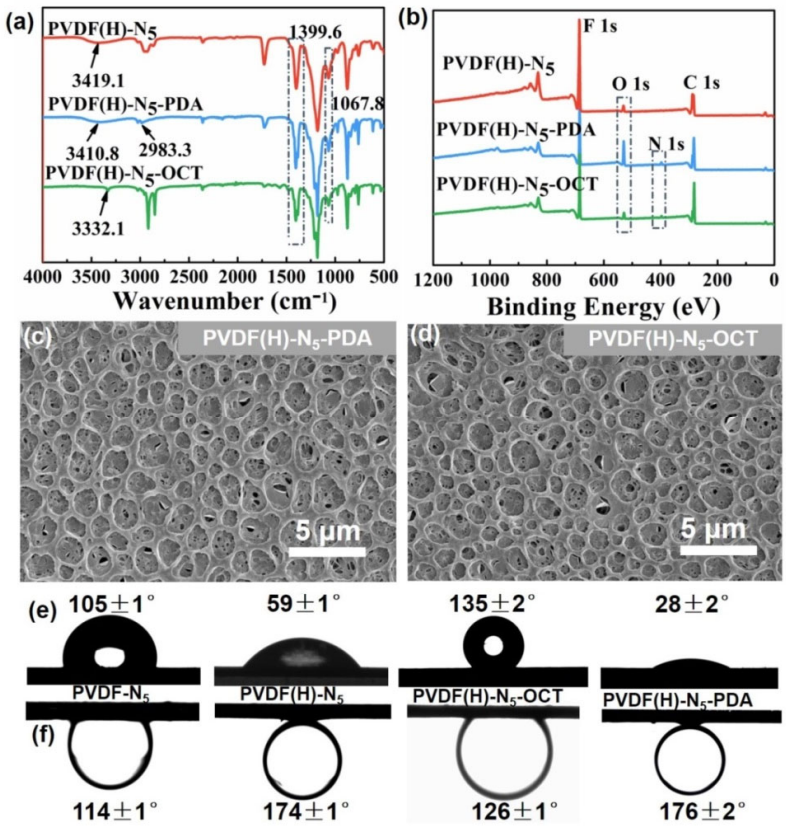

Figure 3. a) ATR-FTIR and b) XPS results of different membranes. SEM images of c) PVDF(H)-N_5-PDA and d) PVDF(H)-N_5-OCT membrane, e) Water contact angle and f) under-water oil contact angle of different membranes.

The *in situ* incorporation of PHEMA controlled the surface tension via the enriched hydroxyl groups. New peaks can be found at 3419 cm^{-1}, 1400 cm^{-1} and 1068 cm^{-1} in ATR-FTIR spectra (Figure 3a), which are attributed to stretching vibration and bending vibration of the hydroxyl groups respectively. [48] The co-existence of PVDF and entangled PHEMA will cause thermodynamic instability and micro-phase separation, which accounts for the formation of dual-scale (micro-/nano-) hyperporous structure. The surface decoration of PDA and OCT can be confirmed by XPS (Figure 3b). Oxygen content increased from 4.3% to 5.2% and also nitrogen element was detected, demonstrating the presence of PDA with catechol and amine groups (Table S1). [49] The further grafting of OCT led to the decrease of fluorine

content from 35.5% to 26.0% and increase of carbon content from 56.7% to 58.5% due to the alkane chain of OCT. [50] In addition, no obvious changes of exterior circular pore structure were found through such an ingenious surface modification strategy (Figure 3c and 3d). The interior porous structure was slightly reduced by PDA coating.

Membrane hydrophilicity governs the interaction between emulsified droplets and membrane surface, therefore influencing the fouling or anti-fouling behavior of membrane. Compared to PVDF-N_5 membrane, wettability of PVDF(H)-N_5 membrane was obviously improved after incorporating hydrophilic PHEMA via *in situ* polymerization (water contact angle decreased from 105 ± 1° to 59 ± 1°, Figure 3e-f). Besides, the enhanced surface roughness (RSa value increased from 0.26 to 0.39 μm, Figure S4) due to the dual-scale micro-/nano- porous surface structure (Figure 2b) combining with in-depth interconnected hyperporous structure (Figure 2e) enhanced the wettability via capillary effect. [51-52] Underwater oil contact angle of PVDF(H)-N_5 membrane was as high as 174 ± 1° (Figure 3e) due to the stable hydrated water layer caused by strong affinity of hydroxyl groups with water. [10] In order to shed light on the effect of suitable hydrophilicity on oil/water separation performance, PVDF(H)-N_5 membrane was further modified to obtain high hydrophilicity (28 ± 2°, Figure 3e) and high hydrophobicity (135 ± 2°, Figure 3e) through polydopamine coating and octadecylamine grafting respectively. The underwater oil contact angle changed to 126 ± 1° for PVDF(H)-N_5-OCT and 176 ± 2° for PVDF(H)-N_5-PDA after surface modification (Figure 3f). It is anticipated that the manipulated surface wettability (hydrophilicity, high hydrophilicity and high hydrophobicity) will influence the transport behavior of oil/water emulsions.

Separation performance of the membranes. Great efforts have been devoted to constructing superwetting interfaces with suppressed adhesion property towards dispersed

phases to accomplish the oil/water emulsion separation. [17, 53-55] However, the so-prepared membranes based on retention mechanism encounter severe fouling due to inevitable deposition of dispersed phases. The rejected emulsified droplets have nowhere to go but are forced onto the membrane surface under hydraulic pressure, which intensifies membrane fouling. Highly hydrophobic surface may cause high affinity towards dispersed phase, thus aggravating the adsorption and fouling issue. Highly hydrophilic surface would repel the dispersed oil phase more efficiently due to the highly hydrated layer, while rejected oil droplets are prone to accumulating on membrane surface to impede the mass transfer as a result. Besides, amphiphilic surfactants would alter the surface wetting properties and decay separation efficiency.

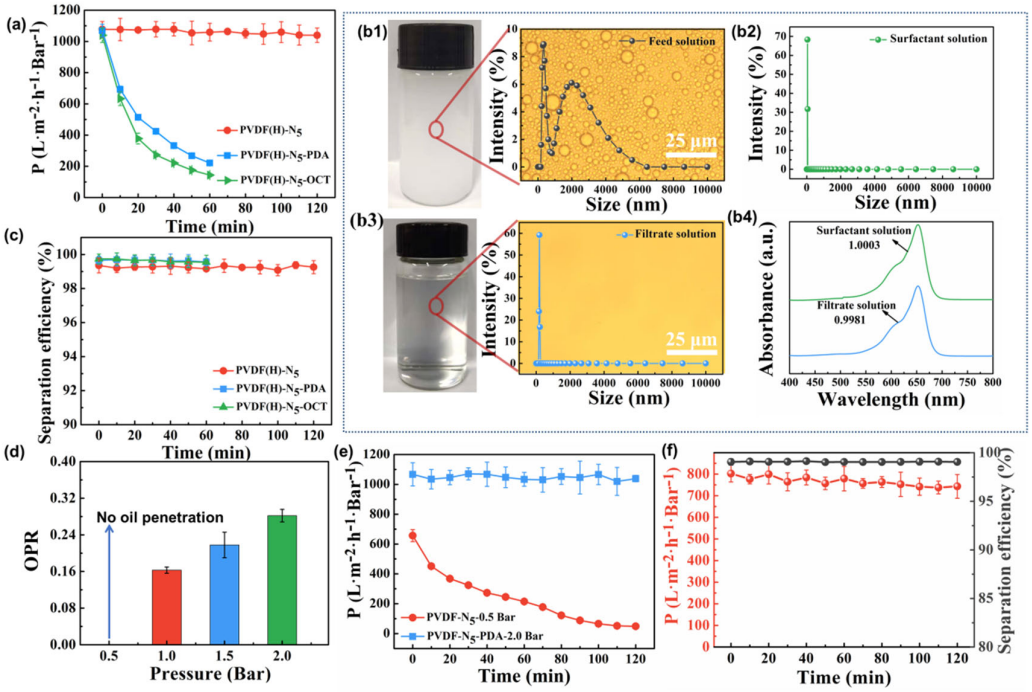

Figure 4. a) Permeability of PVDF(H)-N5, PVDF(H)-N5-PDA and PVDF(H)-N5-OCT for toluene-in-water emulsion under 1.0 bar. b1) the milky emulsion of toluene-in-water shows a bimodal distribution of oil droplets, b2) size distribution of surfactant solution, b3) the permeate is transparent and clear without involving droplets and shows a monodisperse at ~200 nm, b4) the permeate and control surfactant solution shows similar SLS-MB absorbance (detailed method for SLS concentration test can be found in supporting information). d) Oil penetration rate (OPR) of PVDF(H)-N5 at different pressure. e) Permeability of PVDF(H)-N5

at 0.5 bar and PVDF(H)-N_5-PDA at 2.0 bar for treating toluene-in-water emulsion. f) Stable separation performance of PVDF(H)-N_5 for D5-in-water emulsion under 1.0 bar.

We herein show that stable oil/water emulsions were successfully demulsified by the rationally designed membrane. PVDF(H)-N_5 membrane showed a "non-fouling" permeability (1078±50 $Lm^{-2}h^{-1}bar^{-1}$) and separation efficiency (> 99%) in 2 h of continuous cross-flow operation under 1.0 bar (Figure 4a, c). In clear contrast, both highly hydrophobic PVDF(H)-N_5-OCT and hydrophilic PVDF(H)-N_5-PDA displayed declined permeation due to unfavourable interface interaction. Optical microscopy photographs shows the milky emulsion turns to transparent clear solution after membrane filtration (Figure 4b1 and b3). The permeated solution shows a monodispersion at ~200 nm in contrast to bimodal distribution of feed emulsion (Figure 4b1 and b3), which is similar to the surfactant distribution (Figure 4b2). Similar UV absorbance of SLS-MB was also measured for permeate and control surfactant (Figure 4b4). It clearly shows that surfactants for stabilizing the oil droplet were scratched off from the interface membrane and form free or micelle aggregates in permeate. Unlike common superwetting membranes, PVDF(H)-N_5 membrane with dual-scale hyperporous structure and rational wettability allows for coalesced demulsification, and the emulsions go through the membrane and coalesce to free oil phases immiscible to water (see supporting information, VS1). In contrast to conventional superwetting membranes that retain the dispersion phases whose accumulation near the membrane inevitably promotes fouling, the dual-scale hyperporous structure in the current study demulsified the dispersed phases by promotion deformation and coalescence of micro-/nano- dispersed oil droplets in size-matched circular-like pores and confined tortuous channels. The coalesced droplets were growing and accumulating in hyperporous membrane until releasing to form macroscopic phases, which can be easily removed by demixing and delayering.

Hydrodynamics greatly influences the membrane demulsification process. [56] With increasing the hydraulic pressure to 1.0, 1.5 and 2.0 bar, oil penetration rate (OPR) can rise up to 0.16, 0.22 and 0.28, respectively (Figure 4d). Under 0.5 bar, PVDF(H)-N_5 cannot achieve coalesced demulsification, and only water can go through the membrane, leading to a declined water permeability. While highly hydrophilic PVDF(H)-N_5-PDA showed a stable permeability under 2.0 bar (Figure 4e). Membrane fouling was severe for highly hydrophobic PVDF(H)-N_5-OCT despite higher pressure was applied. In addition, D5-in-water emulsion was evaluated for coalesced demulsification in treating highly viscous oily water (5.5-6.5 mPa·s) compared to toluene (0.6 mPa·s). [23] High permeability (750±50 $Lm^{-2}h^{-1}bar^{-1}$) and high separation efficiency (99%) can be stably maintained during the 2-h continuous cross-flow operation (Figure 4f). It is note that no membrane washing was exerted during the whole operation.

The theoretical critical break through pressure (ΔP_b) was calculated to be 2.3 bar according to the following equation: [57]

$$\Delta P_b = \frac{2\gamma cos\theta}{r}$$

where γ is the water-oil interfacial tension (35 mN m^{-1} for water and toluene), θ is the underwater oil contact angle on membrane surface (174 °, as shown in Figure 3) and r is the maximum membrane pore radius (0.3 μm). However, the presence of surfactant would reduce the interfacial tension between water and toluene, [58] which therefore caused a reduced critical pressure. In this case, toluene droplets were able to pass through the membrane at 1.0 bar with the aid of surfactants. With increasing pressure, the coalesced oil phases are prone to releasing from the membrane and alleviating the fouling, which thus gives a stable permeability as well. PVDF(H)-N_0 with mono-dispersed pore size showed declined permeability (Figure S5a) despite its similar hydrophilicity (water contact angle was about 68 °, Figure S5b) with

PVDF(H)-N_5, underpinning the importance of dual-scale hyperporous structure for demulsification. Emulsion size was in the range of 0.1-0.4 μm (Figure 4b1), which is comparable to the primary circular pore size of exterior layer (Figure 2h). The size-matched surface pores tend to capture and disturb the planar flow of emulsions and form turbulent flow, which facilitates the coalescence of dispersed droplets through shearing and collision. The circulated emulsions displayed a floating oil layer on the top (Figure S6), which was ascribed to the surface shearing demulsification. In comparison, no delayering was observed in case of PVDF(H)-N_0 (Figure S6).

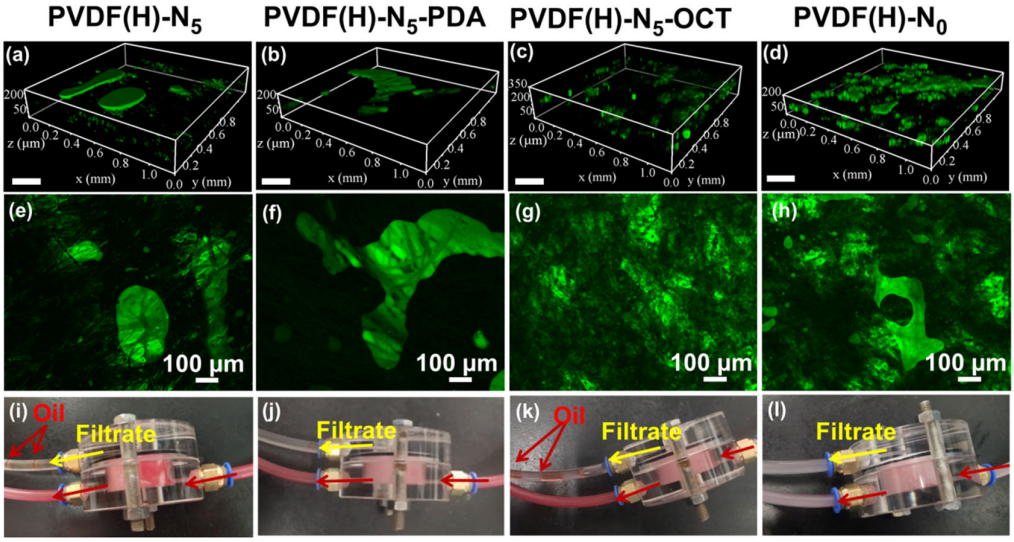

Figure 5. 3D CLSM images of oil phase distribution in (a, e) PVDF(H)-N_5, (b, f) PVDF(H)-N_5-PDA, (c, g) PVDF(H)-N_5-OCT and (d, h) PVDF(H)-N_0. Visual images of the filtrates during cross flow separation. Oil phase was dyed with Sudan III for better identification (i, j, k, l). Scale bars in all 3D CLSM images are all 200 μm.

Coalesced demulsification mechanism. To understand the membrane demulsification behavior, we observed the coalescence phenomenon using dual-channel confocal laser scanning microscopy (Figure 5a-h). Macroscopic oils (green parts) with several hundreds of micrometers can be found in PVDF(H)-N_5 membrane after filtration for 2 h (Figure 5a and 5e), which can freely pass through the membrane with the water flow. Clear oil columns can

be intermittently observed in the filtrate tube (Figure 5i). For PVDF(H)-N_5-PDA membrane, no oil columns were observed in the filtrate (Figure 5j). Coalesced oils were rejected by the superwetting surface (Figure 5b and 5f) and cannot permeate the membrane due to high intrusion pressure. For PVDF(H)-N_5-OCT, most of dispersed oil phases tend to randomly adhere and accumulate in the membrane, thus resulted in the decay of permeability (Figure 4a). Oil Coalescence can also be found in the filtrate tube (Figure 5k). PVDF(H)-N_0 failed to demulsify the filtrate solution due to the absence of hyperporous structure (Figure 5d, 5h and 5k).

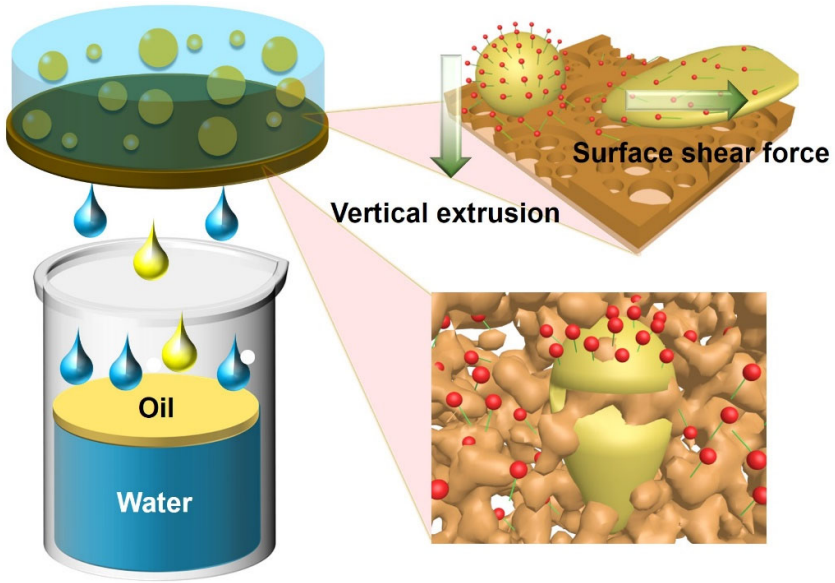

Figure 6. Illustration of the demulsification mechanism at surface and inner of the membrane.

Based on above considerations, beyond superwetting membranes, a membrane with rational surface hydrophilicity and dual-scale hyperporous structure solved the fouling issue of oil/water emulsion through coalescence demulsification. The surface shearing and throat-pore squeezing coalescence mechanism was proposed to elucidate membrane demulsification. The coalescence process can be described as follows: the feed emulsion flows tangentially along the membrane surface, and the size-matched primary circular micropores facilitate fluid turbulent motion via enhanced shearing force to cause breaking up dispersed oils.

Macroscopic coalesced oils were easily flushed away from the membrane surface to form the creaming layer, and big free droplets can penetrate the pore throat and coalesce into macroscopic oil phase via squeezing deformation under hydraulic pressure (Figure 6). [59] While smaller oil droplets were forced into the secondary tortuous pathway under certain pressure. The throat pore can hinder the free transportation of oil droplets and enhance collision coalescence (Figure 7). [60-61] The surfactants were scratched away from the liquid interface film via short range intermolecular interaction including Van der Waals, electrostatic and steric effect in confined pores. The instable droplets were therefore merging and growing to macroscopic oil phases via coalescence and Ostwald ripening. The permeation was therefore composed of two distinct immiscible liquid phases. Therefore, both primary circular pores and secondary throat pores are responsible for shearing and collision coalescence demulsification.

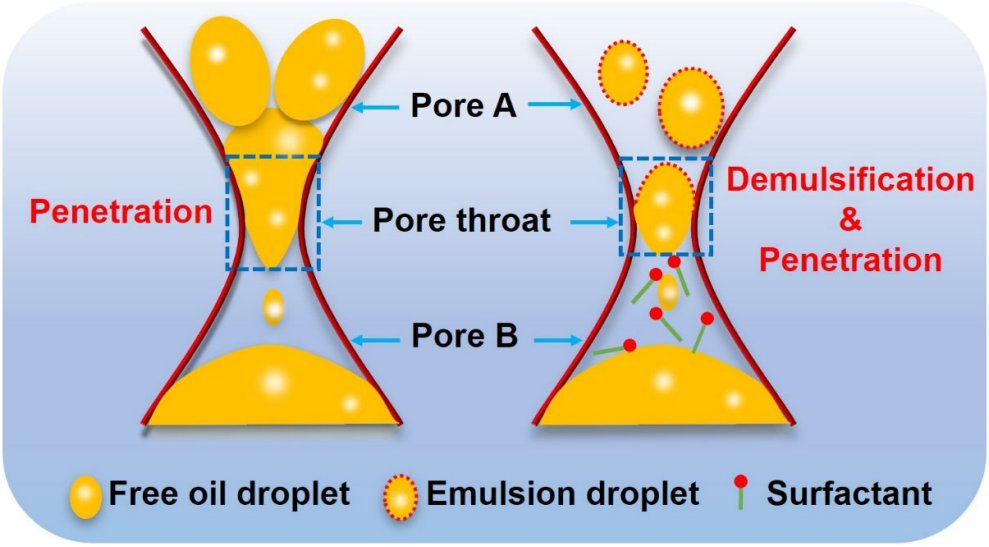

Figure 7. Schematic illustration of coalescence process in membrane pores.

Besides, the surface wettability influenced the fouling issue greatly. In case of a highly hydrophilic surface, more dispersed oils were rejected and the concentrates were accumulating and depositing on the feed side of the membrane to cause severe surface

fouling. However, fouling can be alleviated to some extents by conquering the critical pressure. Highly hydrophobic surface means low penetration pressure for dispersed oils. More dispersed oil droplets were adsorbed and trapped in the tortuous structure and reluctant to be detached from the membrane due to high affinity, which consequently caused irreversible fouling. Thus, rational interface wettability was required to balance the intrusion and removal of emulsified oil droplets in the hyperporous membrane. It can be considered as an "easy come easy go" surface, which is located at "non-fouling" zone 2 in Figure S7.

■ CONCLUSIONS

In this study, PVDF(H)-N_5 membrane was fabricated to achieve "non-fouling" demulsification separation of oil/water via a non-solvent/vapor induced phase separation. The membrane showed a dual-layer hyperporous structure distinctly from common membranes, which was composed of primary exterior circular pores (0.5-2.5 μm) and secondary interior pores (0.1-0.3 μm). The *in situ* polymerization of poly(hydroxyethyl methylacrylate) (PHEMA) endowed the membranes with rational surface wettability (contact angle 59 ± 1°). Filtrates of the membrane for both toluene-in-water and D5-in-water were composed of distinct immiscible liquid phases. PVDF(H)-N_5 membrane showed stable permeability (1078±50 $Lm^{-2}h^{-1}bar^{-1}$) and high separation efficiency (>99.0%) in 2 h of continuous cross flow without physicochemical washing compared to superhydrophilic PVDF(H)-N_5-PDA or highly hydrophobic PVDF(H)-N_5-OCT membranes. The surface shearing and confined pore throat collision were thought to be the coalescence demulsification mechanism. Rational surface wettability allows for "non-fouling" intrusion and removal of emulsified oil droplets, which can be considered as an "easy come easy go" surface. Beyond common superwetting membranes, these findings are of great significance for the practical application of oil/water emulsion separation and fundamental understanding of membrane demulsification.

■ EXPERIMENTAL SECTION

Chemicals and materials. Poly(vinylidene fluoride) (PVDF, FR904) was purchased from Shanghai 3F New Materials Technology Co., LTD (China). 2,2'-Azobis(2-methylpropionitrile) (AIBN, 98%), dopamine hydrochloride (DA, 98%), sodium dihydrogen phosphate monohydrate (≥98%), tris(hydroxymethyl)aminomethane (≥99.7%), sodium laurylsulfonate (SLS, 99%), n-octadecylamine (≥97.0%), methylene blue (Mw = 319.85) and hydroxyethyl methylacrylate (HEMA, 97%) were all obtained from Aladdin (China). Triethyl phosphate (TEP), toluene (≥99.5%), anhydrous ethanol (≥99.7%), sulfuric acid (H_2SO_4, 95.0%~98.0%), hydrochloric acid aqueous solution (HCl, 36.0%~38.0%), trichloromethane (≥99.0%) and sodium hydroxide (NaOH, ≥96.0%) were all purchased from Sinopharm Chemical Reagent Co., Ltd, (China). Decamethylcyclopentasiloxane (D5, ≥97%) was purchased from Trellis Trade Co., Ltd (China). All regents were used as received.

Dual-scale hyperporous membrane fabrication. Dual-scale hyperporous membrane was fabricated via a vapor/non-solvent induced phase separation technique. Typically, homogeneous PVDF/TEP solution (12.5wt %) was prepared by dissolving PVDF in TEP at 80 ^oC with constant stirring for 24 h. The obtained PVDF/TEP solution was deaerated under reduced pressure for 2 h to form casting solution. Then, the solution was casted on PET non-woven fabric (NWF) (80 g m^{-2}) mounted on a glass plate with a casting knife (the gap was setting as 100 μm). The obtained viscous film was then put in a sealed water tank (distance between the film surface and water was kept at about 20 cm) fumigated by hot saturated vapor (90 ^oC) for 5 s for a vapor-induced phase separation (VIPS). After that, the film was immersed in a coagulation bath (V_{Water}: V_{TEP}=1:1) for 0 s, 5 s or 60 s, respectively and then transferred in water at 60 ^oC for 24 h for non-solvent induced phase separation (NIPS). The

corresponding membranes were denoted as PVDF-N_0, PVDF-N_5 and PVDF-N_{60}, respectively. Finally, the fabricated dual-scale hyperporous membranes were dried at room temperature for further use and characterization.

Rationally hydrophilic modification. Dual-scale hyperporous membranes were further modified with *in situ* polymerization of HEMA to construct rationally hydrophilic surface/interface. Hydrophilic monomer HEMA was uniformly dispersed in PVDF/TEP solution, and then *in situ* initiated to form entanglement between PHEMA and PVDF. During the dual phase inversion process, hydrophilic chains can segregate to membrane surfaces and pore interfaces as well to endow the whole membrane with controlled hydrophilicity. Specifically, AIBN (0.4 g) and HEMA (5.5 g) was dissolved in TEP (14.0 g), and then the obtained solution was added into a pre-prepared PVDF/TEP solution (13.5 g PVDF with 80 g TEP) to get the modified casting solution. The casting and solidification processes for modified PVDF membrane were the same as described above. Corresponding membranes were denoted as PVDF(H)-N_0, PVDF(H)-N_5 and PVDF(H)-N_{60}, respectively.

As a control, we also prepared highly hydrophilic and hydrophobic PVDF membranes based on PVDF(H)-N_5 through surface coating of polydopamine (PDA) and surface grafting of octadecylamine respectively. Specifically, PVDF(H)-N_5 membrane was added in dopamine/tris-HCl aqueous solution (2 g L^{-1}) with pH value of 8.5 for 20 min to obtain highly hydrophilic membrane PVDF(H)-N_5-PDA. Subsequently PDA coated membrane was immersed in octadecylamine/alcohol solution (15 mM) for 24 h to obtain highly hydrophobic membrane PVDF(H)-N_5-OCT.

Separation performance of the membranes. A certain amount of anionic surfactant SLS was dissolved in deionized water to form SLS aqueous solution (0.1 g L^{-1}). Then toluene or

D5 was added into the above solution with continuous mechanical stirring for 12 h to prepare stable oil-in-water emulsion (1.0 vol%). The emulsified solutions were kinetically stable, and no creaming, sedimentation or phase separation was observed in 17 h (Figure S1). A home-made cross-flow device was applied to evaluate the oil/water separation performances, where the membrane was mounted in a cell (diameter of 2.8 cm). Feed emulsion was pumped into the cell under a hydraulic pressure (0.5, 1 or 2 bar). The permeation was collected at a time interval of 10 min to calculate membrane permeability. The membrane fabrication and membrane demulsification processes were schematically depicted in Figure 1.

Membrane permeability (P, $Lm^{-2}h^{-1}bar^{-1}$) is calculated through Equation 1:

$$\mathrm{P} = \frac{V}{S \times \Delta t \Delta p}$$

where V (L) is volume of filtrate solution, S (m^2) is the effective membrane area, Δt (h) is the filtration time and Δp (bar) is the applied pressure.

Separation efficiency (Se) is calculated through Equation 2:

$$\mathrm{Se} = \frac{C_f - C_p}{C_f} \times 100\%$$

where C_f (mg L^{-1}) and C_p (mg L^{-1}) is the oil concentration in feed solution and permeate solution respectively. As permeate solution contains demulsified oil phase (top layer) and aqueous phase (bottom layer), C_p is the oil concentration of aqueous solution.

Oil penetration rate (OPR) is determined by Equation 3:

$$\mathrm{OPR} = 1 - \frac{C_f - C_p}{C_f}$$

where C_f (mg L^{-1}) and C_p (mg L^{-1}) is the oil concentration in feed solution and permeate solution respectively. Before testing the oil concentration in permeate solution, the demusified

oil phase (top layer) was ultrasonic dispersed into the permeate solution. Therefore, all the oil phase passed through membrane was calculated into C_p.

Characterizations. Cold field emission scanning electron microscopy (FE-SEM, S4800, Japan) was employed to analyze surface and cross-section morphologies of the membranes with an applied voltage of 4 kV. Before SEM testing, membrane samples were sputter-coated with platinum. Surface hydrophilicity/hydrophobicity was determined by measuring the contact angle with surface tension/dynamic contact angle measuring instrument (TUB 100, Germany). Hydrophobic membranes were firstly washed by ethanol and deionized water before testing its underwater oil contact angle. Chemical compositions of membranes were detected by Intelligent Fourier infrared spectrometer (FTIR, NICOLET 6700, USA). Confocal laser scanning microscope (Leica TCS SP8, Germany) was used to get 3D images of membrane surfaces. In order to get a clear oil distribution in membrane, perylene was used to dye the oil phase. Dynamic light scattering particle size analyzer (ZETA, Zetasizer Nano ZS, UK) was employed to analyze the oil droplet size and its distribution. Total organic carbon analyzer (MultiNC2100, Germany) was employed to measure oil contents in feed emulsions and the corresponding filtrates. Photos of the feed solution and the corresponding filtrates were taken by Polarized optical microscopy (BX51, Japan).

■ ASSOCIATED CONTENT

Supporting information

The Supporting Information is available free of charge at https://pubs.acs.org/doi/XXX.

Method for measuring of concentration of surfactant; video of filtration process of PVDF(H)-N_5 membrane for toluene-in-water emulsion solution; optical photographs of prepared emulsion; cross-section SEM images of PVDF(H)-N_0 and PVDF(H)-N_{60} membrane; SEM images of PVDF-N_0, PVDF-N_5 and PVDF-N_{60} membrane; confocal laser scanning

microscope images of PVDF(H)-N_5 and PVDF-N_5 membrane; permeability of PVDF(H)-N_0 membrane for toluene-in-water emulsion under a applied pressure of 1.0 bar; water contact angle of PVDF(H)-N_0 membrane; optical photographs of oil-in-water emulsion solution after filtration through different membranes; relationships between affinity strength, penetration pressure and surface hydrophilicity of membranes.

■ AUTHOR INFORMATION

Corresponding Authors

Jianqiang Wang-Key Laboratory of Marine Materials and Related Technologies, Zhejiang Key Laboratory of Marine Materials and Protective Technologies, Ningbo Institute of Materials Technology and Engineering, Chinese Academy of Sciences, Ningbo, 315201, P. R. China; University of Chinese Academy of Sciences, Beijing, 100049, P. R. China; orcid.org/0000-0003-3913-1975; E-mail: wangjianqiang@nimte.ac.cn

Fu Liu-Key Laboratory of Marine Materials and Related Technologies, Zhejiang Key Laboratory of Marine Materials and Protective Technologies, Ningbo Institute of Materials Technology and Engineering, Chinese Academy of Sciences, Ningbo, 315201, P. R. China; University of Chinese Academy of Sciences, Beijing, 100049, P. R. China; Chinese Academy of Sciences, Suzhou 215123, China; orcid.org/0000-0003-0041-1873; E-mail: fu.liu@nimte.ac.cn

Authors

Bing He - Key Laboratory of Marine Materials and Related Technologies, Zhejiang Key Laboratory of Marine Materials and Protective Technologies, Ningbo Institute of Materials Technology and Engineering, Chinese Academy of Sciences, Ningbo, 315201, P. R. China; School of Marine Science and Technology, Sino-Europe Membrane Technology Research Institute, Harbin Institute of Technology, Weihai, 264209, P. R. China

Yajie Ding - Key Laboratory of Marine Materials and Related Technologies, Zhejiang Key Laboratory of Marine Materials and Protective Technologies, Ningbo Institute of Materials Technology and Engineering, Chinese Academy of Sciences, Ningbo, 315201, P. R. China;

Tiantian Li - Key Laboratory of Marine Materials and Related Technologies, Zhejiang Key Laboratory of Marine Materials and Protective Technologies, Ningbo Institute of Materials Technology and Engineering, Chinese Academy of Sciences, Ningbo, 315201, P. R. China;

Weilin Zhang - Key Laboratory of Marine Materials and Related Technologies, Zhejiang Key Laboratory of Marine Materials and Protective Technologies, Ningbo Institute of Materials Technology and Engineering, Chinese Academy of Sciences, Ningbo, 315201, P. R. China;

Yingjie Zhang - School of Marine Science and Technology, Sino-Europe Membrane Technology Research Institute, Harbin Institute of Technology, Weihai, 264209, P. R. China

Chuyang Y. Tang - Department of Civil Engineering, The University of Hong Kong, Hong Kong, 999077, P. R. China; orcid.org/0000-0002-7932-6462

Complete contact information is available at:

https://pubs.acs.org/xxx

Author Contributions

J. W.: conceptualization, methodology, investigation, writing- original draft preparation. B. H.: visualization, formal analysis, investigation, writing- original draft preparation. Y. D.: writing - review & editing, formal analysis, investigation. T. L.: data curation, formal analysis, investigation. W. Z.: data curation, formal analysis, investigation. Y. Z.: supervision, methodology. F. L.: conceptualization, writing - review & editing, supervision. C. Y. T.: conceptualization, writing - review & editing.

Notes

The authors declare no competing financial interest.

■ ACKNOWLEDGEMENTS

This work is financially supported by National Nature Science Foundation of China (51661165012), NSFC/RGC Joint Research Scheme sponsored by the Research Grants Council of Hong Kong and the National Natural Science Foundation of China (N_HKU706/16), Zhejiang Provincial Natural Science Foundation of China for Distinguished Young Scholars (LR20E030002), Ten thousand plan-high level talents special support plan of Zhejiang province, China (ZJWR0108020).

■ REFERENCES

(1). Schrope, M., Oil Spill Deep Wounds. *Nature* **2011,** *472* (7342), 152-154.

(2). Shannon, M. A.; Bohn, P. W.; Elimelech, M.; Georgiadis, J. G.; Marinas, B. J.; Mayes, A. M., Science and Technology for Water Purification in the Coming Decades. *Nature* **2008,** *452* (7185), 301-10.

(3). Zhu, Y. Z.; Wang, D.; Jiang, L.; Jin, J., Recent Progress in Developing Advanced Membranes for Emulsified Oil/Water Separation. *Npg Asia Mater.* **2014,** *6*, e101.

(4). Wang, B.; Liang, W.; Guo, Z.; Liu, W., Biomimetic Super-Lyophobic and Super-Lyophilic Materials Applied for Oil/Water Separation: A New Strategy Beyond Nature. *Chem. Soc. Rev.* **2015,** *44* (1), 336-61.

(5). Wang, X.; Yu, J.; Sun, G.; Ding, B., Electrospun Nanofibrous Materials: A Versatile Medium for Effective Oil/Water Separation. *Mater. Today* **2016,** *19* (7), 403-414.

(6). Chu, Z. L.; Feng, Y. J.; Seeger, S., Oil/Water Separation with Selective Superantiwetting/Superwetting Surface Materials. *Angew. Chem., Int. Ed.* **2015,** *54* (8), 2328-2338.

(7). Zhang, F.; Zhang, W. B.; Shi, Z.; Wang, D.; Jin, J.; Jiang, L., Nanowire-Haired Inorganic Membranes with Superhydrophilicity and Underwater Ultralow Adhesive Superoleophobicity for High-Efficiency Oil/Water Separation. *Adv. Mater.* **2013,** *25* (30), 4192-4198.

(8). Kota, A. K.; Kwon, G.; Choi, W.; Mabry, J. M.; Tuteja, A., Hygro-Responsive Membranes for Effective Oil-Water Separation. *Nat Commun* **2012,** *3*, 1025.

(9). Zhu, Y.; Wang, J.; Zhang, F.; Gao, S.; Wang, A.; Fang, W.; Jin, J., Zwitterionic Nanohydrogel Grafted Pvdf Membranes with Comprehensive Antifouling Property and Superior Cycle Stability for Oil-in-Water Emulsion Separation. *Adv. Funct. Mater.* **2018,** *28* (40), 1804121.

(10). He, B.; Ding, Y.; Wang, J.; Yao, Z.; Qing, W.; Zhang, Y.; Liu, F.; Tang, C. Y., Sustaining Fouling Resistant Membranes: Membrane Fabrication, Characterization and Mechanism Understanding of Demulsification and Fouling-Resistance. *J. Membr. Sci.* **2019,** *581*, 105-113.

(11). Tang, C. Y.; Chong, T. H.; Fane, A. G., Colloidal Interactions and Fouling of Nf and Ro Membranes: A Review. *Adv. Colloid Interface Sci.* **2011,** *164* (1–2), 126-143.

(12). Lu, D. W.; Zhang, T.; Ma, J., Ceramic Membrane Fouling During Ultrafiltration of Oil/Water Emulsions: Roles Played by Stabilization Surfactants of Oil Droplets. *Environ. Sci. Technol.* **2015,** *49* (7), 4235-4244.

(13). Chen, X. S.; Wen, G.; Guo, Z. G., What Are the Design Principles, from the Choice of Lubricants and Structures to the Preparation Method, for a Stable Slippery Lubricant-Infused Porous Surface? *Mater. Horiz.* **2020,** *7* (7), 1697-1726.

(14). Wu, J.; Wei, W.; Li, S.; Zhong, Q.; Liu, F.; Zheng, J.; Wang, J., The Effect of Membrane Surface Charges on Demulsification and Fouling Resistance During Emulsion Separation. *J. Membr. Sci.* **2018,** *563*, 126-133.

(15). Lv, Y.; Ding, Y.; Wang, J.; He, B.; Yang, S.; Pan, K.; Liu, F., Carbonaceous Microsphere/Nanofiber Composite Superhydrophilic Membrane with Enhanced Anti-Adhesion Property Towards Oil and Anionic Surfactant: Membrane Fabrication and Applications. *Sep. Purif. Technol.* **2020,** *235*, 116189.

(16). Padaki, M.; Surya Murali, R.; Abdullah, M. S.; Misdan, N.; Moslehyani, A.; Kassim, M. A.; Hilal, N.; Ismail, A. F., Membrane Technology Enhancement in Oil–Water Separation. A Review. *Desalination* **2015,** *357*, 197-207.

(17). Zhao, Y. H.; Zhang, M.; Wang, Z. K., Underwater Superoleophobic Membrane with Enhanced Oil-Water Separation, Antimicrobial, and Antifouling Activities. *Adv. Mater. Interfaces* **2016,** *3* (13), 1500664.

(18). Feng, L.; Li, S. H.; Li, Y. S.; Li, H. J.; Zhang, L. J.; Zhai, J.; Song, Y. L.; Liu, B. Q.; Jiang, L.; Zhu, D. B., Super-Hydrophobic Surfaces: From Natural to Artificial. *Adv. Mater.* **2002,** *14* (24), 1857-1860.

(19). Wong, T. S.; Kang, S. H.; Tang, S. K. Y.; Smythe, E. J.; Hatton, B. D.; Grinthal, A.; Aizenberg, J., Bioinspired Self-Repairing Slippery Surfaces with Pressure-Stable Omniphobicity. *Nature* **2011,** *477* (7365), 443-447.

(20). Zhang, W.; Zhu, Y.; Liu, X.; Wang, D.; Li, J.; Jiang, L.; Jin, J., Salt-Induced Fabrication of Superhydrophilic and Underwater Superoleophobic Paa-G-Pvdf Membranes for Effective Separation of Oil-in-Water Emulsions. *Angew. Chem., Int. Ed.* **2014,** *53* (3), 856-60.

(21). Ge, P.; Wang, S. L.; Zhang, J. H.; Yang, B., Micro-/Nanostructures Meet Anisotropic Wetting: From Preparation Methods to Applications. *Mater. Horiz.* **2020,** *7* (10), 2566-2595.

(22). Zhu, Z.; Wang, W.; Qi, D.; Luo, Y.; Liu, Y.; Xu, Y.; Cui, F.; Wang, C.; Chen, X., Calcinable Polymer Membrane with Revivability for Efficient Oily-Water Remediation. *Adv. Mater.* **2018,** *30* (30), 1801870.

(23). Wu, J.; Ding, Y.; Wang, J.; Li, T.; Lin, H.; Wang, J.; Liu, F., Facile Fabrication of Nanofiber- and Micro/Nanosphere-Coordinated Pvdf Membrane with Ultrahigh Permeability of Viscous Water-in-Oil Emulsions. *J. Mater. Chem. A* **2018,** *6* (16), 7014-7020.

(24). Liao, Y.; Tian, M.; Wang, R., A High-Performance and Robust Membrane with Switchable Super-Wettability for Oil/Water Separation under Ultralow Pressure. *J. Membr. Sci.* **2017,** *543*, 123-132.

(25). Yang, X. B.; Sun, H. G.; Pal, A.; Bai, Y. P.; Shao, L., Biomimetic Silicification on Membrane Surface for Highly Efficient Treatments of Both Oil-in-Water Emulsion and Protein Wastewater. *ACS Appl. Mater. Interfaces* **2018,** *10* (35), 29982-29991.

(26). Yuan, T.; Meng, J. Q.; Hao, T. Y.; Wang, Z. H.; Zhang, Y. F., A Scalable Method toward Superhydrophilic and Underwater Superoleophobic Pvdf Membranes for Effective Oil/Water Emulsion Separation. *ACS Appl. Mater. Interfaces* **2015,** *7* (27), 14896-14904.

(27). Wei, C. J.; Dai, F. Y.; Lin, L. G.; An, Z. H.; He, Y.; Chen, X.; Chen, L.; Zhao, Y. P., Simplified and Robust Adhesive-Free Superhydrophobic Sio2-Decorated Pvdf Membranes for Efficient Oil/Water Separation. *J. Membr. Sci.* **2018,** *555*, 220-228.

(28). Qing, W.; Shi, X.; Zhang, W.; Wang, J.; Wu, Y.; Wang, P.; Tang, C. Y., Solvent-Thermal Induced Roughening: A Novel and Versatile Method to Prepare Superhydrophobic Membranes. *J. Membr. Sci.* **2018,** *564*, 465-472.

(29). Ding, Y.; Wu, J.; Wang, J.; Wang, J.; Ye, J.; Liu, F., Superhydrophilic Carbonaceous-Silver Nanofibrous Membrane for Complex Oil/Water Separation and Removal of Heavy Metal Ions, Organic Dyes and Bacteria. *J. Membr. Sci.* **2020,** *614*, 118491.

(30). Cai, Y. H.; Chen, D. Y.; Li, N. J.; Xu, Q. F.; Li, H.; He, J. H.; Lu, J. M., A Self-Cleaning Heterostructured Membrane for Efficient Oil-in-Water Emulsion Separation with Stable Flux. *Adv. Mater.* **2020,** *32* (25), 2001265.

(31). Wei, C. J.; Lin, L. G.; Zhao, Y. P.; Zhang, X. Y.; Yang, N.; Chen, L.; Huang, X. J., Fabrication of Ph-Sensitive Superhydrophilic/Underwater Superoleophobic Poly(Vinylidene

Fluoride)-Graft-(Sio2 Nanoparticles and Pamam Dendrimers) Membranes for Oil-Water Separation. *ACS Appl. Mater. Interfaces* **2020,** *12* (16), 19130-19139.

(32). Gao, S.; Zhu, Y.; Wang, J.; Zhang, F.; Li, J.; Jin, J., Layer-by-Layer Construction of Cu2+/Alginate Multilayer Modified Ultrafiltration Membrane with Bioinspired Superwetting Property for High-Efficient Crude-Oil-in-Water Emulsion Separation. *Adv. Funct. Mater.* **2018,** *28* (49), 1801944.

(33). Ding, Y.; Wu, J.; Wang, J.; Lin, H.; Wang, J.; Liu, G.; Pei, X.; Liu, F.; Tang, C. Y., Superhydrophilic and Mechanical Robust Pvdf Nanofibrous Membrane through Facile Interfacial Span 80 Welding for Excellent Oil/Water Separation. *Appl. Surf. Sci.* **2019,** *485*, 179-187.

(34). Yang, X. B.; Sun, P.; Zhang, H. R.; Xia, Z. J.; Waldman, R. Z.; Mane, A. U.; Elam, J. W.; Shao, L.; Darling, S. B., Polyphenol-Sensitized Atomic Layer Deposition for Membrane Interface Hydrophilization. *Adv. Funct. Mater.* **2020,** *30* (15), 1910062.

(35). Wang, R. X.; Zhao, X. T.; Jia, N.; Cheng, L. J.; Liu, L. F.; Gao, C. J., Superwetting Oil/Water Separation Membrane Constructed from in Situ Assembled Metal-Phenolic Networks and Metal-Organic Frameworks. *ACS Appl. Mater. Interfaces* **2020,** *12* (8), 10000-10008.

(36). Yang, H. C.; Hou, J.; Chen, V.; Xu, Z. K., Janus Membranes: Exploring Duality for Advanced Separation. *Angew. Chem., Int. Ed.* **2016,** *55* (43), 13398-13407.

(37). Wang, Z. X.; Yang, X. B.; Cheng, Z. J.; Liu, Y. Y.; Shao, L.; Jiang, L., Simply Realizing "Water Diode" Janus Membranes for Multifunctional Smart Applications. *Mater. Horiz.* **2017,** *4* (4), 701-708.

(38). Li, T.; Liu, F.; Zhang, S.; Lin, H.; Wang, J.; Tang, C. Y., Janus Polyvinylidene Fluoride Membrane with Extremely Opposite Wetting Surfaces Via One Single-Step Unidirectional Segregation Strategy. *ACS Appl. Mater. Interfaces* **2018,** *10* (29), 24947-24954.

(39). Wang, Z. J.; Liu, G. J.; Huang, S. S., In Situ Generated Janus Fabrics for the Rapid and Efficient Separation of Oil from Oil-in-Water Emulsions. *Angew. Chem., Int. Ed.* **2016,** *55* (47), 14610-14613.

(40). Wang, Z. J.; Lehtinen, M.; Liu, G. J., Universal Janus Filters for the Rapid Separation of Oil from Emulsions Stabilized by Ionic or Nonionic Surfactants. *Angew. Chem., Int. Ed.* **2017,** *56* (42), 12892-12897.

(41). An, Y.-P.; Yang, J.; Yang, H.-C.; Wu, M.-B.; Xu, Z.-K., Janus Membranes with Charged Carbon Nanotube Coatings for Deemulsification and Separation of Oil-in-Water Emulsions. *ACS Appl. Mater. Interfaces* **2018,** *10* (11), 9832-9840.

(42). Daiminger, U.; Nitsch, W.; Plucinski, P.; Hoffmann, S., Novel Techniques for Oil-Water Separation. *J. Membr. Sci.* **1995,** *99* (2), 197-203.

(43). Kocherginsky, N. M.; Tan, C. L.; Lu, W. F., Demulsification of Water-in-Oil Emulsions Via Filtration through a Hydrophilic Polymer Membrane. *J. Membr. Sci.* **2003,** *220* (1-2), 117-128.

(44). Hu, D.; Li, X. Y.; Li, L.; Yang, C. F., Designing High-Caliber Nonwoven Filter Mats for Coalescence Filtration of Oil/Water Emulsions. *Sep. Purif. Technol.* **2015,** *149*, 65-73.

(45). Wang, F.; Altschuh, P.; Ratke, L.; Zhang, H. D.; Selzer, M.; Nestler, B., Progress Report on Phase Separation in Polymer Solutions. *Adv. Mater.* **2019,** *31* (26), 1806733.

(46). Tao, M. M.; Liu, F.; Xue, L. X., Hydrophilic Poly(Vinylidene Fluoride) (Pvdf) Membrane by in Situ Polymerisation of 2-Hydroxyethyl Methacrylate (Hema) and Micro-Phase Separation. *J. Mater. Chem.* **2012,** *22* (18), 9131-9137.

(47). Wang, J.; Wu, Z.; Li, T.; Ye, J.; Shen, L.; She, Z.; Liu, F., Catalytic Pvdf Membrane for Continuous Reduction and Separation of P -Nitrophenol and Methylene Blue in Emulsified Oil Solution. *Chem. Eng. J.* **2018,** *334*, 579-586.

(48). Zhang, G. L.; Lu, S. F.; Zhang, L.; Meng, Q.; Shen, C.; Zhang, J. W., Novel Polysulfone Hybrid Ultrafiltration Membrane Prepared with Tio2-G-Hema and Its Antifouling Characteristics. *J. Membr. Sci.* **2013,** *436*, 163-173.

(49). Wang, J.; Guo, H.; Shi, X.; Yao, Z.; Qing, W.; Liu, F.; Tang, C. Y., Fast Polydopamine Coating on Reverse Osmosis Membrane: Process Investigation and Membrane Performance Study. *J. Colloid Interface Sci.* **2019,** *535*, 239-244.

(50). Chowdhury, M. R.; Steffes, J.; Huey, B. D.; McCutcheon, J. R., 3d Printed Polyamide Membranes for Desalination. *Science* **2018,** *361* (6403), 682-685.

(51). Gao, X.; Jiang, L., Water-Repellent Legs of Water Striders. *Nature* **2004,** *432*, 36.

(52). Li, F.; Wang, Z.; Huang, S.; Pan, Y.; Zhao, X., Flexible, Durable, and Unconditioned Superoleophobic/Superhydrophilic Surfaces for Controllable Transport and Oil-Water Separation. *Adv. Funct. Mater.* **2018,** *28* (20), 1706867.

(53). Jiang, G.; Zhang, S.; Zhu, Y.; Gao, S.; Jin, H.; Luo, L.; Zhang, F.; Jin, J., Hydrogel-Embedded Tight Ultrafiltration Membrane with Superior Anti-Dye-Fouling Property for Low-Pressure Driven Molecule Separation. *J. Mater. Chem. A* **2018,** *6*, 2927.

(54). Cai, Y. H.; Chen, D. Y.; Li, N. J.; Xu, Q. F.; Li, H.; He, J. H.; Lu, J. M., A Smart Membrane with Antifouling Capability and Switchable Oil Wettability for High-Efficiency Oil/Water Emulsions Separation. *J. Membr. Sci.* **2018,** *555*, 69-77.

(55). Sun, Y.; Lin, Y.; Fang, L.; Zhang, L.; Cheng, L.; Tomohisa, Y.; Matsuyama, H., Facile Development of Poly(Tetrafluoride Ethylene-R-Vinylpyrrolidone) Modified Pvdf Membrane with Comprehensive Antifouling Property for Highly-Efficient Challenging Oil-in-Water Emulsions Separation. *J. Membr. Sci.* **2019,** *584*, 161-172.

(56). Hlavacek, M., Break-up of Oil-in-Water Emulsions Induced by Permeation through a Microfiltration Membrane. *J. Membr. Sci.* **1995,** *102*, 1-7.

(57). Chen, P. C.; Xu, Z. K., Mineral-Coated Polymer Membranes with Superhydrophilicity and Underwater Superoleophobicity for Effective Oil/Water Separation. *Sci. Rep.* **2013,** *3*, 2776.

(58). Hong, X.; Huang, X. J.; Gao, Q. L.; Wu, H. M.; Guo, Y. Z.; Huang, F.; Fang, F.; Huang, H. T.; Chen, D. J., Microstructure-Performance Relationships of Hollow-Fiber Membranes with Highly Efficient Separation of Oil-in-Water Emulsions. *J. Appl. Polym. Sci.* **2019,** *136* (23), 47615.

(59). Darvishzadeh, T.; Tarabara, V. V.; Priezjev, N. V., Oil Droplet Behavior at a Pore Entrance in the Presence of Crossflow: Implications for Microfiltration of Oil-Water Dispersions. *J. Membr. Sci.* **2013,** *447*, 442-451.

(60). Wang, H.; Zinchenko, A. Z.; Davis, R. H., The Collision Rate of Small Drops in Linear Flow-Fields. *J. Fluid. Mech.* **1994,** *265*, 161-188.

(61). Hudson, S. D.; Jamieson, A. M.; Burkhart, B. E., The Effect of Surfactant on the Efficiency of Shear-Induced Drop Coalescence. *J. Colloid Interface Sci.* **2003,** *265* (2), 409-421.